

---

# Towards Desynchronization Detection in Biosignals

---

**Akara Supratak**  
Imperial College London  
as12212@ic.ac.uk

**Steffen Schneider**  
Technical University of Munich  
steffen.schneider@tum.de

**Hao Dong**  
Imperial College London  
hao.dong11@ic.ac.uk

**Ling Li**  
University of Kent  
c.li@kent.ac.uk

**Yike Guo\***  
Imperial College London  
y.guo@ic.ac.uk

## Abstract

This study presents a novel data-driven approach to detect desynchronization among biosignals from two modalities. We propose to train a deep neural network to learn synchronized patterns between biosignals from two modalities by transcribing signals from one modality into their expected, simultaneous or synchronized signal in another modality. Thus, instead of measuring the degree of synchrony between signals from *different* modalities using traditional linear and non-linear measures, we simplify this problem into the problem of measuring the degree of synchrony between the real and the synthesized signals from the *same* modality using the traditional measures. Desynchronization detection is then achieved by applying a threshold function to the estimated degree of synchrony. We demonstrate the approach with the detection of eye-movement artifacts in a public sleep dataset and compare the detection performance with traditional approaches.

## 1 Introduction

Estimating degree of synchrony between signals is a common step in the analysis of biological data. Detecting desynchronization among biosignals from multiple modalities can provide useful information in addition to the analysis of each modality separately. By observing significant changes in biosignals from multiple modalities, we may learn more useful insights about the signals. For instance, healthy subjects normally show a sign of synchronized behaviors across different biosignals such as body temperature, heart rate, respiratory rate, and electrophysiological measures. Being able to detect desynchronization across modalities may be used as an early sign of harmful diseases. Traditionally, the degree of synchrony can be quantified by calculating the linear correlation between two signals [1, 2], measuring the amount of information obtained from one signal through another [3], or estimating the synchronization in phase regardless of the signal amplitudes [4]. However, the main purpose of these techniques is to discover and quantify the linear and non-linear relationships among biosignals. Without prior knowledge, it is not straightforward to define features of the signals that can be used to detect desynchronization. Also, there may be non-trivial mappings between biosignals from multiple modalities that can cause commonly used synchronization methods to miss important relationships between the signals.

We propose a novel data-driven approach to detect desynchronization among biosignals from two modalities (or domains). Our approach is to train a model to learn the relationships between biosignals from two domains by transcribing signals from one domain into their expected, simultaneous or synchronized representations in another domain. Desynchronization detection is then achieved by computing the degree of synchrony between the measured (or real) and the transcribed (or synthesized)

---

\*Corresponding Author

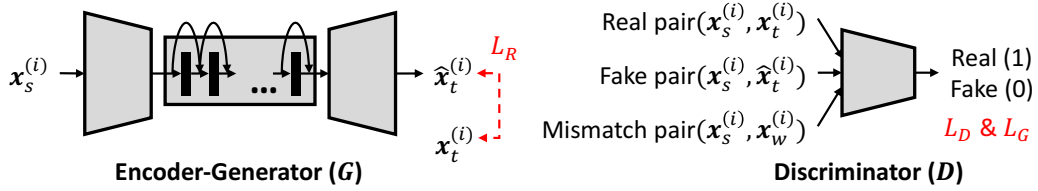


Figure 1: The encoder-generator network  $G$  transcribes signals from the source domain  $S$  to its simultaneous signals in the target domain  $T$ ,  $G : \mathbf{x}_s^{(i)} \rightarrow \hat{\mathbf{x}}_t^{(i)}$ . The discriminator network  $D$  determines whether the input simultaneous signals from both domains are real or fake,  $D : (\mathbf{x}_s^{(i)}, \mathbf{x}_t^{(i)} | \hat{\mathbf{x}}_t^{(i)} | \mathbf{x}_w^{(i)}) \rightarrow \{0, 1\}$ .  $\mathbf{x}_s^{(i)}$  denotes the  $i$ -th epoch from  $S$ .  $\mathbf{x}_t^{(i)}$  denotes the  $i$ -th epoch from  $T$ .  $\hat{\mathbf{x}}_t^{(i)}$  denotes the synthesized, simultaneous signal in  $T$ .  $\mathbf{x}_w^{(i)}$  denotes the mismatch epoch randomly selected from  $T$  (which is not the same as  $\mathbf{x}_t^{(i)}$ ).  $\mathbf{x}_s^{(i)} \in \mathbb{R}^{n_s}$  and  $\mathbf{x}_t^{(i)}, \hat{\mathbf{x}}_t^{(i)}, \mathbf{x}_w^{(i)} \in \mathbb{R}^{n_t}$ , where  $n_s$  and  $n_t$  are the number of data points in each epoch from  $S$  and  $T$  respectively.  $L_D$ ,  $L_G$  and  $L_R$  are losses used during the training. Note that the  $D$  network is only used during training to provide useful gradients for synthesizing the expected, simultaneous signals, and is not used during the signal transcription.

signals using the traditional measures. If the degree of synchrony is less than a given threshold, it is very likely that the desynchronization (i.e., the anomaly) is happening. To our knowledge, this is the first work to transform the problem of detecting desynchronization among biosignals from different modalities into a *simpler* problem of quantifying the degree of synchrony between biosignals from the same modality.

## 2 Cross-domain signal transcription

The key challenge to build a signal transcription model is to learn feature representations that are transferable across modalities. Generative Adversarial Networks (GANs) [5] have recently shown promising results in modeling complex multimodal data and synthesizing realistic images in image to image [6, 7] and text-to-image [8, 9] domain transfer settings. We propose to employ a GAN to build a cross-domain signal transcription model, consisting of a *encoder-generator* and a *discriminator* network as depicted in Figure 1.

We train the model by alternating between gradient descent steps on  $D$  and  $G$ . The  $D$  network is trained to distinguish between real and synthesized pairs of simultaneous biosignals from two domains. The  $G$  network is trained to transcribe  $\mathbf{x}_s^{(i)}$  into  $\hat{\mathbf{x}}_t^{(i)}$  such that it can fool the  $D$  network. Thus there are two training losses  $L_D$  and  $L_G$ , in which  $L_G$  is minimized over  $G$  and  $L_D$  is minimized over  $D$ . Suppose there is a set of  $m$  simultaneously recorded biosignals from  $S$  and  $T$ ,  $\{(\mathbf{x}_s^{(i)}, \mathbf{x}_t^{(i)})\}_{i=1}^m$ , the losses  $L_D$  and  $L_G$  are defined as follows:

$$L_D = - \sum_{i=1}^m \log D(\mathbf{x}_s^{(i)}, \mathbf{x}_t^{(i)}) - \sum_{i=1}^m \log(1 - D(\mathbf{x}_s^{(i)}, G(\mathbf{x}_s^{(i)}))) - \sum_{i=1}^m \log(1 - D(\mathbf{x}_s^{(i)}, \mathbf{x}_w^{(i)})) \quad , \quad (1)$$

$$L_G = - \sum_{i=1}^m \log D(\mathbf{x}_s^{(i)}, G(\mathbf{x}_s^{(i)})) + \alpha L_R \quad . \quad (2)$$

The first two terms in  $L_D$  and the first term in  $L_G$  are the adversarial losses that can guide  $G$  to synthesize simultaneous biosignals in  $T$ . However, it has been shown in [8] that these two terms are not sufficient to train the cross-domain model as the discriminator only observes two kinds of pairs: the real simultaneous signals  $(\mathbf{x}_s^{(i)}, \mathbf{x}_t^{(i)})$ , and the real and synthesized simultaneous signals  $T$ ,  $(\mathbf{x}_s^{(i)}, \hat{\mathbf{x}}_t^{(i)})$ . Therefore, the third term in  $L_D$  is added to enforce the  $G$  network to synthesize  $\hat{\mathbf{x}}_t^{(i)}$  that do not only have the same properties as signals in  $T$ , but also have synchronized behaviors with the given  $\mathbf{x}_s^{(i)}$ . The  $L_R$  term in  $L_G$  is the reconstruction loss which can also help the  $G$  network to synthesize  $\hat{\mathbf{x}}_t^{(i)}$  that look similar to  $\mathbf{x}_t^{(i)}$ . In our work, the mean-squared-error (MSE),  $\|\mathbf{x}_t^{(i)} - \hat{\mathbf{x}}_t^{(i)}\|_2^2$ , is used as the reconstruction loss. Herein,  $\alpha$  is a hyperparameter that controls the strength of the  $L_R$ .

### 3 Desynchronization Detection

As our transcription model learns synchronized relationships between two modalities from the training set, we hypothesize that the model can synthesize the expected, simultaneous biosignals that are similar to the measured ones when there is a sufficient amount of simultaneous pairs from two domains in the training set. Therefore, when the model observes signals that do not sufficiently appear in the training set, such as desynchronized signals (i.e., outlier cases or anomalies), the synthesized signals can be expected to differ from the measured ones.

Formally, each  $i$ -th pair of the real and synthesized biosignals,  $(\mathbf{x}_t^{(i)}, \hat{\mathbf{x}}_t^{(i)})$  is classified as the synchronized (0) or the desynchronized (1) class if:

$$d^{(i)} = \begin{cases} 1, & \text{if } \phi(\mathbf{x}_t^{(i)}, \hat{\mathbf{x}}_t^{(i)}) < \varepsilon \\ 0, & \text{otherwise} \end{cases}, \quad (3)$$

where  $d^{(i)}$  is the desynchronization label of the  $i$ -th epoch of simultaneous signals,  $\phi$  is a function that quantify the degree of synchrony between  $\mathbf{x}_t^{(i)}$  and  $\hat{\mathbf{x}}_t^{(i)}$ , and  $\varepsilon$  is the threshold used to distinguish between the synchronized and the desynchronized signals. As we are trying to measure the similarity between the real and the synthesized biosignals, amplitude correlation is necessary. We propose to use the Pearson’s R coefficient [2],  $r$ , as the function  $\phi$  in Equation 3. The resulting coefficient  $r(\mathbf{x}_t^{(i)}, \hat{\mathbf{x}}_t^{(i)}) \in [-1, 1]$  is an estimate for the linear correlation between the real and the synthesized simultaneous signals. If the value approaches +1,  $\mathbf{x}_t^{(i)}$  and  $\hat{\mathbf{x}}_t^{(i)}$  are considered as being synchronized. If the value approaches -1, they are considered as being desynchronized.

### 4 Results

**Dataset.** We evaluate the desynchronization detection performance using the public sleep dataset from the subset 3 of the cohort 1 from the MASS dataset [10]. It consists of simultaneous recordings from 62 healthy subjects, including two EOG (left and right) and three EEG signals from Fz-CLE, Cz-CLE and Oz-CLE channels (i.e., EEG-Fz, EEG-Cz, and EEG-Oz). The EEG-Fz, EEG-Cz, and EEG-Oz are from the scalp electrodes positioned at the front, central and the back of the head respectively. These signals have the sampling rate of 256 Hz. Each 30-s epoch of these recordings is annotated with one of the five sleep stages: W, N1, N2, N3, and REM.

**Experimental design.** We assume that “eye-movements” are “desynchronization” events. Thus the recordings from the sleep stages that contains eye-movements, which is REM, are annotated as the eye class (i.e., the desynchronized class), while the recordings from the sleep stages that do not contain or only contain a few eye-movements, which are N2 and N3, are annotated as the no-eye class (i.e., the synchronized class). We randomly split the subjects into two sets: 50 subjects for training and validation, and 12 subjects for testing. Only the recordings from the no-eye class are used to train the transcription model. The transcription model was trained to transcribe each 5-s epoch of two EOG signals (i.e.,  $n_s = 256 \cdot 5$ ) into its expected, simultaneous 5-s epoch of EEG-Fz signal (i.e.,  $n_t = 256 \cdot 5$ ). The trained model is then applied to all recordings (both the eye and no-eye classes) from the test set. The synthesized 5-s EEG-Fz epochs were aggregated back into 30-s epochs following how each epoch was initially annotated in the dataset for the evaluation.

**Performance metrics.** We evaluate the detection performance using detection accuracy (ACC), F1-score (F1), sensitivity or true positive rate (TPR), false positive rate (FPR), and area under the ROC curve (AUC). These metrics are used to compare the detection performance with baseline approaches, which will be discussed below.

**Baseline methods.** We compare the performance of desynchronization detection with two baseline methods: Pearson’s R coefficient (BASE-1) and intrinsic phase synchrony [11] (BASE-2). For each method, we directly compute the degree of synchrony among 30-s epochs of simultaneous EOG and EEG signals without the synthesized signals. Specifically, we estimate the degree of synchrony of three pairs: EOG (left) - EOG (right), EOG (left) - EEG Fz, and EOG (right) - EEG Fz. The degrees of synchrony from all pairs were summarized via averaging. The averaged value from each 30-s epoch was compared with a given threshold to detect desynchronization.

**Desynchronization detection performance.** Table 1 shows a comparison between our proposed and the two baseline methods across degree of synchrony of each class, ACC, F1, and AUC. The

Table 1: Comparison between our proposed and the baseline methods across degree of synchrony of each class, detection accuracy (ACC), F1-score (F1), and area under ROC curves (AUC).

| Method   | Test Epochs |      | Degree of Synchrony |                 | $\epsilon$ | Performance Metrics |              |             |
|----------|-------------|------|---------------------|-----------------|------------|---------------------|--------------|-------------|
|          | No-eye      | Eye  | No-eye              | Eye             |            | ACC                 | F1           | AUC         |
| BASE-1   | 7579        | 1904 | $0.45 \pm 0.13$     | $0.34 \pm 0.09$ | 0.39       | 67.87               | 49.31        | 0.73        |
| BASE-2   | 7579        | 1904 | $0.04 \pm 0.01$     | $0.05 \pm 0.03$ | 0.04       | 47.89               | 23.62        | 0.40        |
| Proposed | 7579        | 1904 | $0.49 \pm 0.13$     | $0.33 \pm 0.13$ | 0.42       | <b>70.64</b>        | <b>51.16</b> | <b>0.80</b> |

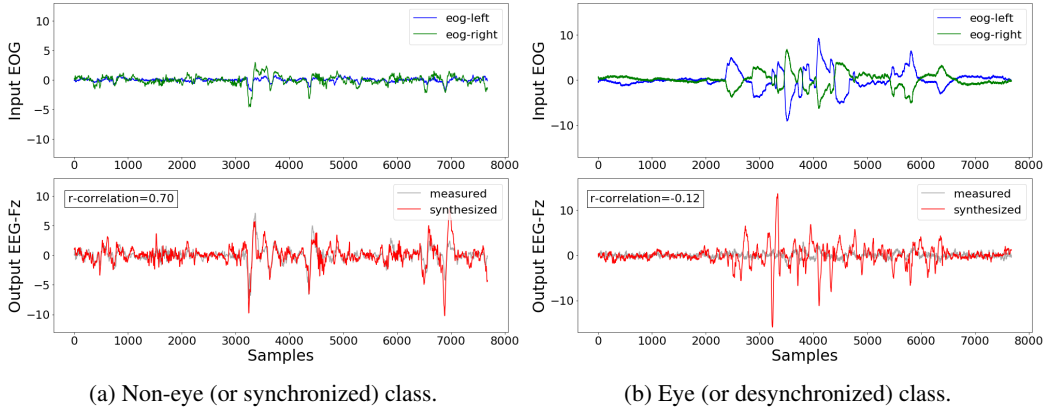


Figure 2: Examples of 30-s epochs of EEG-Fz signals synthesized from 30-s epochs of EOG signals from (a) the no-eye and (b) the eye class from one subject. It can be seen that the  $r$  correlation (i.e., the degree of synchrony) between the real and the synthesized signals is high (0.70) for the no-eye epoch and low (-0.12) for the eye epoch.

numbers in bold indicate the highest performance metrics of all methods. The  $\epsilon$  thresholds used to distinguish between the no-eye and the eye classes in Equation 3 were selected from the ones that gave the best performance in term of TPR and FPR (i.e.,  $\epsilon$  that gave TPR and FPR closest to the perfect classification point, TPR=1 and FPR=0, in terms of Euclidean distance).

It can be seen that our method achieved a better performance compared to the baseline methods. These results showed that using the linear correlation alone (BASE-1) was not sufficient to capture the relationships among multiple signals from different modalities. Some important information may be lost because the degree of synchrony was quantified by averaging the correlations from all pairs. Thus our transcription model can help capturing such relationships and preventing the loss of information from averaging the degree of synchrony from all pairs. The results also demonstrated that, without prior knowledge about the desynchronized patterns presented in the dataset, it is not straightforward to apply phase synchronization (BASE-2) to distinguish between the no-eye and the eye epochs. This is because we do not know in advance which frequency bands should be compared. Thus learning the synchronized (or common) patterns from the training data can simplify the process of manually hand-engineering synchronized features, which can be labor-intensive, time-consuming and application-specific.

## 5 Conclusions

We propose a novel data-driven approach to detect desynchronization between biosignals from two modalities. We demonstrate that our cross-domain signal transcription model can help capturing the relationships between EOG and EEG signals that were missed by the traditional Pearson’s R coefficient approaches. We also found that the phase synchronization method requires prior knowledge about the frequency bands that are useful for eye-movement detection. This shows that our approach simplifies the problem of “detecting desynchronization among biosignals from different modalities” into the problem of “comparing the similarity between the real and the synthesized signals from the same modality”.

## References

- [1] R. N. Bracewell, *The Fourier transform and its applications*. McGraw-Hill, New York, 1965.
- [2] K. A. Bollen and K. H. Barb, "Pearson's R and Coarsely Categorized Measures," *American Sociological Review*, vol. 46, no. 2, pp. 232–239, 1981.
- [3] T. M. Cover and J. A. Thomas, *Elements of Information Theory 2nd Edition*. Wiley, 2006.
- [4] F. Varela, J.-p. Lachaux, E. Rodriguez, and J. Martinerie, "The brainweb: phase synchronization and large-scale integration," *Nature Reviews Neuroscience*, vol. 2, no. 4, pp. 229–239, 2001.
- [5] I. Goodfellow, J. Pouget-Abadie, M. Mirza, B. Xu, D. Warde-Farley, S. Ozair, A. Courville, and Y. Bengio, "Generative Adversarial Nets," *Advances in Neural Information Processing Systems (NIPS)*, pp. 2672–2680, 2014.
- [6] Y. Taigman, A. Polyak, and L. Wolf, "Unsupervised Cross-Domain Image Generation," *Iclr*, 2017.
- [7] P. Isola, J.-Y. Zhu, T. Zhou, and A. A. Efros, "Image-to-Image Translation with Conditional Adversarial Networks," *arXiv preprint*, p. 16, 2016.
- [8] S. Reed, Z. Akata, X. Yan, L. Logeswaran, B. Schiele, and H. Lee, "Generative Adversarial Text to Image Synthesis," *Icml*, pp. 1060–1069, 2016.
- [9] H. Zhang, T. Xu, H. Li, S. Zhang, X. Huang, X. Wang, and D. Metaxas, "StackGAN: Text to Photo-realistic Image Synthesis with Stacked Generative Adversarial Networks," *arXiv preprint*, 2016.
- [10] C. O'Reilly, N. Gosselin, J. Carrier, and T. Nielsen, "Montreal Archive of Sleep Studies: an open-access resource for instrument benchmarking and exploratory research," *Journal of Sleep Research*, vol. 23, no. 6, pp. 628–635, 2014.
- [11] D. Looney, A. Hemakom, and D. P. Mandic, "Intrinsic multi-scale analysis: a multi-variate empirical mode decomposition framework," *Proceedings of the Royal Society A: Mathematical, Physical and Engineering Sciences*, vol. 471, no. 2173, 2014.